Contents

1. Introduction

The ***standard model of particle*** is the theory that describe all the elementary particles, the electroweak [**PhysRevLett.19.1264**] and the strong interaction

2. Hadron-Hadron Scattering

In a high energy proton-proton collision we can have either soft or hard processes. Most of the time the hard processes are accompanied by soft interaction, occurring along the hadron interaction. The hard processes are well understood using perturbation theory, meanwhile the soft processes are not so well understood in fact these processes are described by non perturbative QCD.

2.1 QCD factorization theorem

The factorization theorem was introduced first by Drell and Yan (ref: S.D. Drell and T.M. Yan, Ann. Phys. 66 (1971) 578.).

The hadron-hadron scattering is describe in terms of partons extending the formalism used for deep inelastic scattering.

$$\sigma_{AB} = \int dx_a\, dx_b\, f_{a/A}(x_a)\, f_{b/B}(x_b)\, \hat{\sigma}_{ab\to X} \tag{2.1}$$

Where X is a partonic/leptonic state and $a\,(b)$ a quark or an antiquark in the hadron $A\,(B)$. This is valid in the "scaling" limit:

$$s \longrightarrow \infty \qquad\qquad \frac{M_X}{s} = \text{finite} \tag{2.2}$$

The problem arise from the perturbative corrections from real and virtual gluon emission. This contribution give a logarithmic divergence (spoil the convergence of the perturbative expansion). These dependencies can be absorbed by the parton distribution function (DGLAP equations). This result in the violation of scaling:

$$f_{a/A}(x_a) \longrightarrow f_{a/A}(x_a, Q^2) \tag{2.3}$$

Now the parton distribution function depend on the momentum scale Q^2.

So, we can rewrite the factorization theorem in Eq. 2.1 as:

$$\sigma_{AB} = \int dx_a\, dx_b\, f_{a/A}(x_a, Q^2)\, f_{b/B}(x_b, Q^2)\, \hat{\sigma}_{ab\to X} \tag{2.4}$$

Now the *finite* corrections in the perturbative expansion are specific for each process (not universal). This leads in the Eq. 2.4 to the α_s series:

$$\sigma_{AB} = \int dx_a\, dx_b\, f_{a/A}(x_a, \mu_F^2)\, f_{b/B}(x_b, \mu_F^2)\, \left[\hat{\sigma}_0 + \alpha_s(\mu_R^2)\hat{\sigma}_1 + \dots\right] \tag{2.5}$$

In Eq. 2.5 two scales enter the formula:

– The *factorization scale* μ_F: this scale separates long- and short- distance.

– The *renormalization scale* μ_R: the scale at which is evaluated the strong coupling α_s.

The higher-order corrections eliminate the cross section prediction dependencies on μ_R and μ_F. Typically, the scales are assumed to be equal. For example in the Drell-Yan process the standard choice is $\mu_F = \mu_R = M$, with M the lepton pair mass.

The parton distribution functions used in the hard scattering are solution of the DGLAP (Dokshitzer–Gribov–Lipatov–Altarelli–Parisi) equation:

$$\mu_F^2 \frac{\partial f_{i/H}(x,\mu_F^2)}{\partial \mu_F^2} = \sum_j \frac{\alpha_s(\mu_F^2)}{2\pi} \int_x^1 \frac{dz}{z} P_{i\to j}(z)\ f_{j/p}\left(\frac{x}{z}, \mu_F^2\right) \tag{2.6}$$

Where $P_{i\to j}$ are the splitting functions: they are the probability to have a parton of type i that became, by the emission of a quark or a gluon, a parton j, carrying fraction z of the momentum of i.

The splitting functions have perturbative expansions:

$$P_{i\to j}(x,\alpha_s) = P^{(0)}_{i\to j}(x) + \frac{\alpha_s}{2\pi} P^{(1)}_{i\to j}(x) + \dots \tag{2.7}$$

This procedure has been used to calculate Standard Model cross section in $p\overline{p}$ and pp scattering respectively at Tevatron and LHC energies as shown in Fig. 2.1.

The parton distribution functions dependence on Q^2 can be derived theoretically via the DGLAP equations. While, the x dependence is given fitting the deep-inelastic and other hard-scattering processes experimental data. The experimental coverage in (x, Q^2)-plane is shown in Fig. 2.2 where is also underlined the relationship between (x, Q^2) and kinematic variables in Drell-Yan processes for a final state with invariant mass M and rapidity y is shown. Assuming that the factorization scale Q is equal to M (The reference center of mass energy is 13 TeV). So, for two incoming particles with four-momentum respectively p_1 and p_2 the relations with y and M are:

$$\begin{aligned} p_1^\mu &= \frac{\sqrt{s}}{2}(x_1, 0, 0, x_1) \\ p_2^\mu &= \frac{\sqrt{s}}{2}(x_2, 0, 0, -x_2) \end{aligned} \quad \Longrightarrow \quad x_1 = \frac{M}{\sqrt{s}} e^{y} \qquad x_2 = \frac{M}{\sqrt{s}} e^{-y} \tag{2.8}$$

where $s = (p_1^\mu + p_2^\mu)^2$.

2.2 Partonic cross section

Partonic cross section is one of the fundamental ingredients in our recipe. This can be calculated in a perturbative series in α_s from QCD first principles using quantum field theory.

The calculation at the leading order (LO) is performed evaluating all the possible tree-level Feynman diagrams for every process. Evaluating the squared matrix element and integrating over the available phase space (analytically or numerically).

Already, here we can encounter some divergence that have to be avoided imposing restriction on the phase space.

2.2.1 Higher order calculations

The LO calculation can describe broad feature of a particular process and provide a first estimation of its cross section but in many cases this is insufficient.

The main source of uncertainty derives from the LO dependence on the unphysical renormalization and factorization scales. Some process may contribute only when going beyond the first approximation, and some divergence can be resummed.

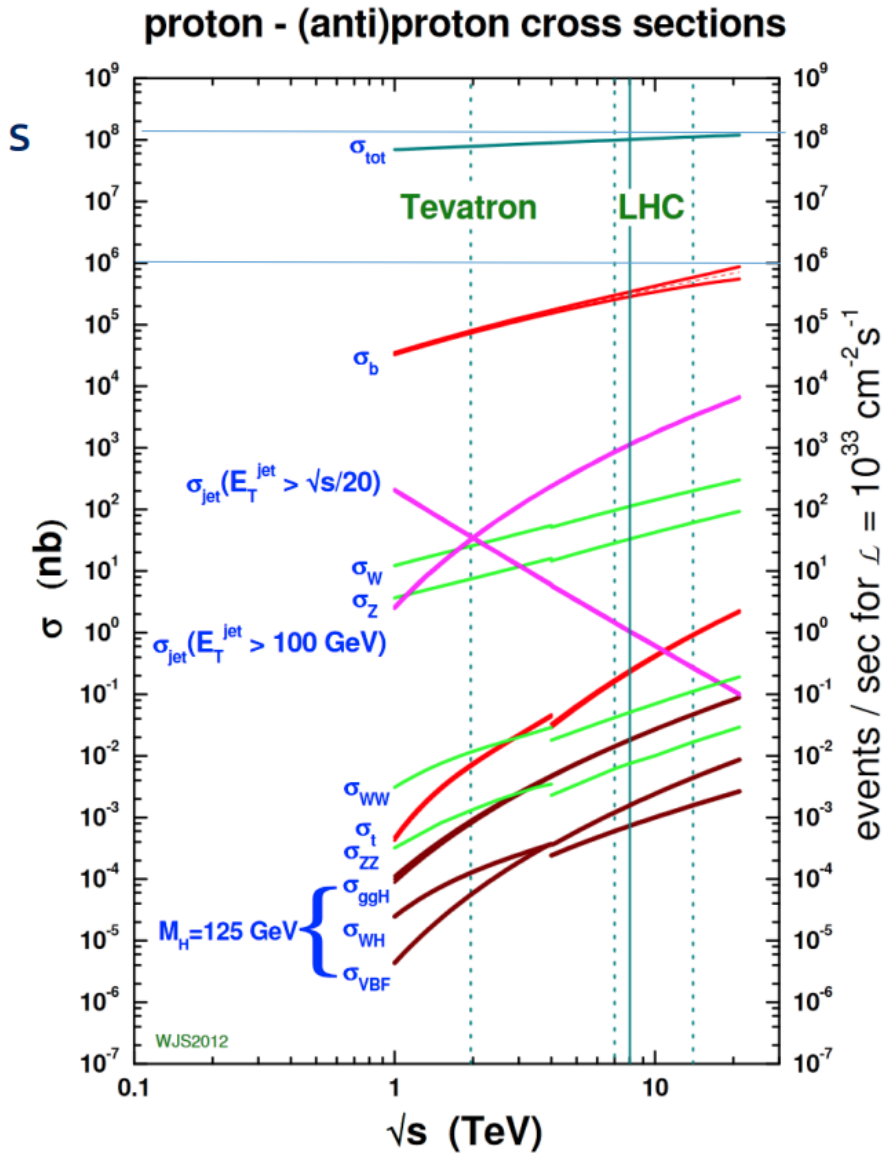

Figure 2.1: Next-to-leading order cross sections at Tevatron and LHC colliders energies (the splitting are at the transition between $p\bar{p}$ and pp cross section). Figure from (S. Catani, hep-ph/0005233)

To the next-to-leading orer (NLO) calculation participate all the Feynman diagrams that take an extra α_s. This contribution can arise in two different way:

- Virtual: internal lines (loops);
- Real: external lines (real particles).

Virtual corrections contains infrared divergences, arising from the integral on the loop circulating momentum, that cancel against infrared singularities given by collinear emissions or soft emissions.

A common strategy for the rinormalization is dimensional regularization: consists into perform the calculation in a $D = 4 - 2\epsilon$-dimensional space ($\epsilon < 0$), in that way the singularities appear as single and double poles in ϵ. Than, the limit $\epsilon \to 0$ is taken after the divergences have cancelled.

This NLO calculation with regularization allows to extend the treatment to zero transverse momentum.

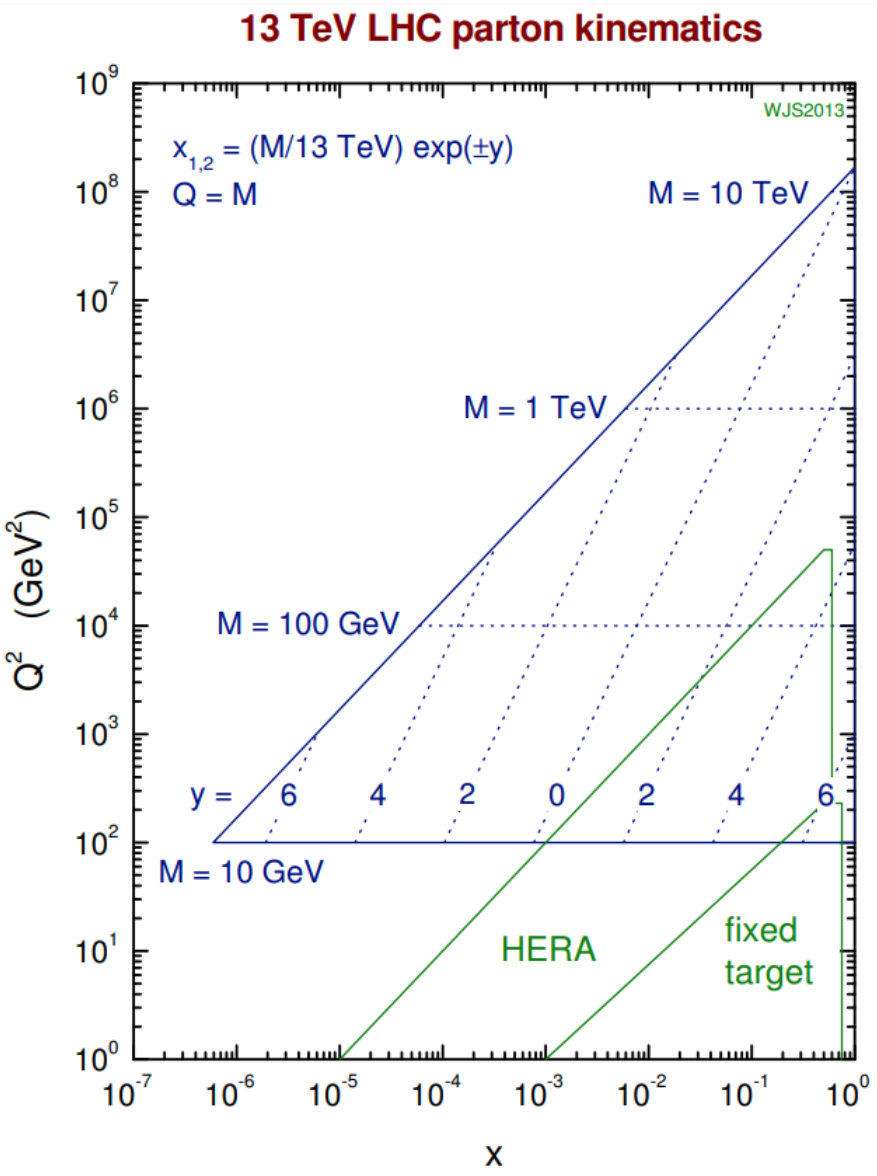

Figure 2.2: Graphical representation of the parton (x, Q^2) variables coverage of different experiments. For LHC these x and Q^2 are related to the kinematic variables y and M

The importance of higher order calculations can be seen with the following example. In a Z boson production:

1) **LO**: the Z is produced without transverse momentum (p_T), anything can recoil against the Z for momentum conservation.

2) **NLO**: the Z acquire a finite p_T, in this case the Z boson p_T is balanced by a single parton/gluon.

3) **NNLO**: the Z p_T can be balanced by two jets.

Another important benefit of performing a NLO calculation is the the reduction of the dependence on the unphysical renormalization (μ_R) and factorization (μ_F) scales. It is proven that higher order calculations is that observables calculated to order α_s^n are dependent on the unphysical scales only at order higher than α_s^{n+1}. The range of predictions corresponding to different scale choices is usually attributed to *theoretical uncertainties*.

2.3 Parton Showers

A different approach, instead than calculating order by order in the perturbative expansion, is to use an *all-order* approach in order to describe the phenomena observed at high-energy colliders.

different all-order approaches exist e.g. resummation and parton showers. Resummation is based on the observation that in many quantities the smallness of the expansion coefficients α_s is violated by large logarithmic enhancements. This take the dominant contribution from each order and "resum" them by means of an evolution equation. The main problem in QCD is related to the fact that lot of quantities have correction of the form $\alpha_s^n \log^k(Q_i/Q_j)$ where Q_i and Q_f are two different energies scales, for example:

– Renormalization and factorization scales logs: $\alpha_s^n \log^n(Q^2/\mu_f)$

Various methods to perform this resummation exist.

An other *all-order* approach is parton showers, this is implemented in different programs PYTHIA, HERWIG and SHERPA. This start from few parton arising from hard interaction and than these are related to partons to a lower energy scale close to Λ_{QCD} using the DGLAP evolution equation formalism, the solution at this equation can be write using a Sudakov form factor arising from the probability of no gluon emission in the evolution from higher scale to lower scale.

An example is the Z production p_T spectrum shown in Fig. 2.3. A comparison between experimental CDF data and theoretical predictions is shown: in the low p_T region the *all-order* approach regularize the divergence of the fixed order calculation and describe the data better then the last one.

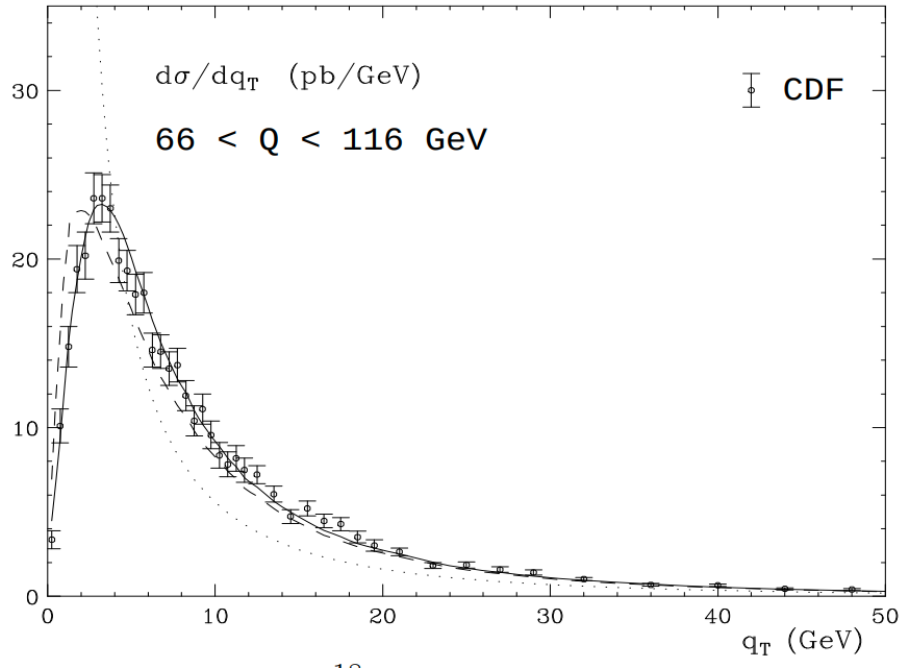

Figure 2.3: CDF data on Z production cross section at Tevatron collider, CDF experiment, the predictions from fixed order calculation (dotted) with resummation (dashed), and with the inclusion of power corrections (solid) are compared (preso da A. Kulesza et al., hep-ph/0207148)

3. Multiple Parton Interactions

The fact that the hadrons are viewed as "bunches" of partons it is likely that in an hadron-hadron different couples of partons can undergo to a scattering. This phenomenon is know as Multiple Parton Interactions (MPI) and is related to the composite nature of the incoming hadrons.

So, at some level these MPI have to exist, and are important in the description of the event: They can change the color topology of the colliding system as a whole,

In this scenario it is important to have a good understanding of the phenomenon. The aim of this section is to describe the basic concepts that are use to simulate MPI, for example in `Pythia` Monte Carlo event generator.

3.1 Basic Concepts

The main hypothesis of the multiple interaction models is that the QCD factorization is true not only for the hard process but also for the other scatters.

So, we can write:

$$\frac{d\sigma_{\text{int}}}{dp_\perp} = \sum_{i,j,k,l} \int dx_1 \int dx_2 \int d\hat{t}\, f_i(x_1, Q^2) f_j(x_2, Q^2) \frac{d\hat{\sigma}_{ij\to kl}}{d\hat{t}} \delta\left(p_\perp^2 - \frac{\hat{t}\hat{u}}{\hat{s}}\right) \tag{3.1}$$

This is the differential cross section for QCD hard $2 \to 2$ processes, this processes are the one reported in Table 3.1.

In Eq. 3.1 we use the Mandelstam variables associated to the partonic system:

$$\hat{s} = (p_1 + p_2)^2 = (p_3 + p_4)^2 = x_1 x_2 s \tag{3.2}$$

$$\hat{t} = (p_1 - p_3)^2 = (p_2 - p_4)^2 \tag{3.3}$$

$$\hat{u} = (p_1 - p_4)^2 = (p_2 - p_3)^2 \tag{3.4}$$

wherer p_1, p_2 are the four-momenta of the incoming partons and p_3, p_4 the four-momenta of the outgoing partons. Note that in Eq. 3.1 the jet cross section is twice as large $\sigma_{\text{jet}} = 2\sigma_{\text{int}}$, because at first approximation each interaction give rise to two jets.

We assume also that the "hardness" of processes is defined by the $p_\perp$ scale of the interaction ($Q^2 = p_\perp^2$).

As you can see from the formulae in Table 3.1 at small scattering angles: for $t \to 0$, the t-channel gluon exchange processes $qq' \to qq'$, $qg \to qg$ and $gg \to gg$ dominate the full matrix element. For scattering that are soft relative to $\hat{s}$, $|\hat{t}| \ll \hat{s}$, we can approximate $|\hat{t}|$ as:

$$p_T^2 = \frac{\hat{t}\hat{u}}{\hat{s}} = \frac{\hat{t}(-\hat{s} - \hat{t})}{\hat{s}} \approx |\hat{t}| \tag{3.5}$$

In this limit the only difference between quark and gluon are the color factors:

$$\hat{\sigma}_{gg} : \hat{\sigma}_{qg} : \hat{\sigma}_{qq} = \frac{9}{4} : 1 : \frac{4}{9} \tag{3.6}$$

Process	Partonic cross section
$q\,q' \rightarrow q\,q'$	$\frac{4}{9}\frac{\hat{s}^2+\hat{u}^2}{\hat{t}^2}$
$q\,q \rightarrow q\,q$	$\frac{4}{9}\left(\frac{\hat{s}^2+\hat{u}^2}{\hat{t}^2}+\frac{\hat{s}^2+\hat{t}^2}{\hat{u}^2}\right)-\frac{8}{27}\frac{\hat{s}^2}{\hat{u}\hat{t}}$
$q\,\overline{q} \rightarrow q'\,\overline{q}'$	$\frac{4}{9}\frac{\hat{s}^2+\hat{u}^2}{\hat{t}^2}$
$q\,\overline{q} \rightarrow q\,\overline{q}$	$\frac{4}{9}\left(\frac{\hat{s}^2+\hat{u}^2}{\hat{t}^2}+\frac{\hat{t}^2+\hat{u}^2}{\hat{s}^2}\right)-\frac{8}{27}\frac{\hat{u}^2}{\hat{s}\hat{t}}$
$q\,\overline{q} \rightarrow g\,g$	$\frac{32}{27}\frac{\hat{t}^2+\hat{u}^2}{\hat{t}\hat{u}}-\frac{8}{3}\frac{\hat{t}^2+\hat{u}^2}{\hat{s}^2}$
$g\,g \rightarrow q\,\overline{q}$	$\frac{1}{6}\frac{\hat{t}^2+\hat{u}^2}{\hat{t}\hat{u}}-\frac{8}{3}\frac{\hat{t}^2+\hat{u}^2}{\hat{s}^2}$
$g\,q \rightarrow g\,q$	$-\frac{4}{9}\frac{\hat{s}^2+\hat{u}^2}{\hat{s}\hat{u}}-\frac{\hat{u}^2+\hat{s}^2}{\hat{t}^2}$
$g\,g \rightarrow g\,g$	$\frac{9}{2}\left(3-\frac{\hat{t}\hat{u}}{\hat{s}^2}-\frac{\hat{s}\hat{u}}{\hat{t}^2}-\frac{\hat{s}\hat{t}}{\hat{u}^2}\right)$

Table 3.1: Parton-Parton differential cross sections ($2 \rightarrow 2$ QCD process), can beh calculated in pQCD evaluating the matrix element for each process involving quark, antiquark and gluon.

So the Eq. 3.1 can be rewritten as:

$$\frac{d\sigma_{int}}{dp_T^2} \approx \int\int \frac{dx_1}{x_1}\,\frac{dx_2}{x_2}\,F(x_1,p_T^2)\,F(x_2,p_T^2)\frac{d\hat{\sigma}_{2\rightarrow 2}}{dp_T^2} \tag{3.7}$$

whit:

$$\frac{d\hat{\sigma}_{2\rightarrow 2}}{dp_T^2} = \frac{8\pi\alpha_s^2(p_T^2)}{9p_T^4} \tag{3.8}$$

$$F(x,Q^2) = \sum_q \left(x\,q(x,Q^2) + x\,\overline{q}(x,Q^2)\right) + \frac{9}{4}\,x\,g(x,Q^2) \tag{3.9}$$

So we can integrate the Eq. 3.7:

$$\sigma_{int}(p_{T\,min}) = \int_{p_{T\,min}^2}^{(\sqrt{s}/2)^2} \frac{d\hat{\sigma}_{2\rightarrow 2}}{dp_T^2}\,dp_T^2 \propto \frac{1}{p_{T\,min}^2} \xrightarrow{p_{T\,min}\rightarrow 0} \infty \tag{3.10}$$

The total cross section is divergent in the limit $p_T \rightarrow 0$, this divergence is shown in Fig. 3.1. Due to this divergence the total interaction cross section at some p_T scale can exceed the total proton-proton cross section.

- To understand this paradox should be noted that the interaction cross section described in Eq. 3.10 is related to the interaction probability between two partons and counts the number of interactions, while the total proton-proton cross section σ_{pp} counts the number of events. For example, an event (a proton-proton collision) in which two partons interact counts once in the total cross section and twice in the interaction cross section.

So the ratio between this two quantities is perfectly allowed to be larger than unity:

$$\frac{\sigma_{int}(p_{T\,min})}{\sigma_{tot}} = \langle n\rangle(p_T\,min) \tag{3.11}$$

Secondly, we have to consider the screening effect: in fact the incoming hadrons are color singlet objects. Therefore , when the p_T of an exchanged gluon is small, and so the associated

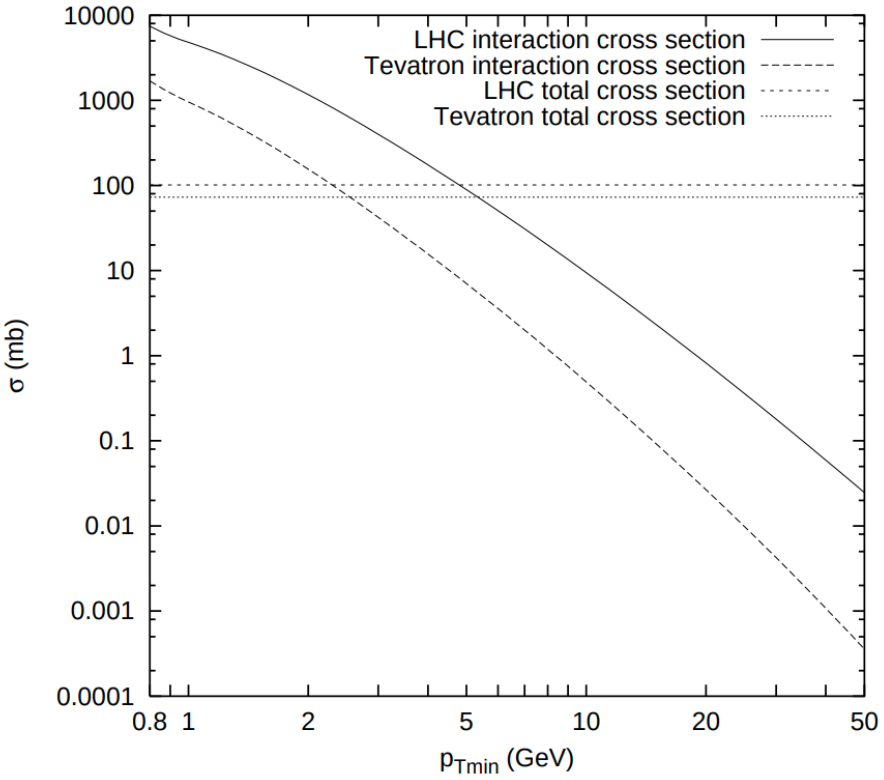

Figure 3.1: ADD caption

wavelength large, this gluon can no longer resolve the color charges and the effective coupling is decreased.

This cutoff is associated with color screening distance i.e. the average size of the region within the compensation of color charge occurs. This cutoff is then introduced in the factor:

$$\frac{\alpha_s^2\left(p_{T0}^2+p_T^2\right)}{\alpha_s^2\left(p_T^2\right)}\frac{p_T^4}{(p_{T0}^2+p_T^2)^2} \tag{3.12}$$

This factor contains the phenomenological regularization of the divergence , with the factor p_{T0} that have to be tuned to data.

Now the interaction cross section i

This parameter p_{T0} do not have to be energy-independent. But the energy is related with the sensibility of our probe, higher energy is related with the capacity of probing PDF to lower x values, this low x region the number of partons rapidly increases. So, the partons are closer packed is this regions and as a consequence the color screening distance d decrease.

The number of partons is related to x with a power low so it is likely to have a dependence of the same form for p_{T0} respect to the CM energy.

$$p_{T0}(\sqrt{s}) = p_{T0}^{ref}\left(\frac{\sqrt{s}}{E_{CM}^{ref}}\right)^{E_{CM}^{pow}} \tag{3.13}$$

3.2 Pythia8 Monte Carlo events generator

Pythia8 is a standard tool for the simulation of events in high energy collisions. Pythia contains the evolution from a few-body system to a complex multiparticle final state.

3.2.1 Parton Shower

In Pythia8 all the contributions from Initial State Radiation (ISR), Final State Radiation (FSR) and Multi Parton Interactions (MPI) are interleaved into a single common sequence of decreasing p_T.

The shower evolution is based on the standard (LO) DGLAP splitting kernels P(z)

$$P_{q\to qg}(z) = C_F \frac{1+z^2}{1-z} \tag{3.14}$$

$$P_{g\to gg}(z) = C_A \frac{(1-z(1-z))^2}{z(1-z)} \tag{3.15}$$

$$P_{q\to q\bar{q}}(z) = T_R(z^2+(1-z)^2) \tag{3.16}$$

where $C_F = \frac{4}{3}$, $C_A = N_C = 3$ and $T_R = \frac{1}{2}$ multiplied by N_f if summing over all contributing quark flavours.

Both ISR and FSR algorithms are based on these splitting kernels.

The probabilities of emitting radiation as one moves in the common downward evolution are:

$$\frac{d\mathcal{P}_{FSR}}{dp_T^2} = \frac{1}{p_T^2}\int dz\,\frac{\alpha_s}{2\pi}P(z) \tag{3.17}$$

$$\frac{d\mathcal{P}_{ISR}}{dp_T^2} = \frac{1}{p_T^2}\int dz\,\frac{\alpha_s}{2\pi}P(z)\,\frac{f'(x/z,p_T^2)}{z\,f(x,p_T^2)} \tag{3.18}$$

3.2.2 Multiple Parton Interactions in Pythia

The MPI, as said before, are also generated in a decreasing p_T sequence. So the hardest MPI is generated first. Than we can write the probability for an interaction, i, to occur at a scale p_T using a Sudakov-type expression:

$$\frac{d\mathcal{P}_{MPI}}{dp_T} = \frac{1}{\sigma_{ND}}\frac{d\sigma_{2\to 2}}{dp_T}\ \exp\left(-\int_{p_T}^{p_T\,i-1}\frac{1}{\sigma_{ND}}\frac{d\sigma_{2\to 2}}{dp'_T}\,dp'_T\right) \tag{3.19}$$

3.2.3 Momentum and flavour conservation

One problem is to achieve momentum conservation, so we need to take into account the modification in the PDF by the $i-1$ interaction. To do that in Pythia the PDF are rescaled to the remaining available x range, adjusting their normalization.

We need to take into account the momentum fraction x_i removed from the hadron remnant by the $i-th$ interaction. This is done evaluating PDF not at x_i but at a rescaled value

$$x'_i = \frac{x_i}{X} \qquad \text{with:} \quad X = 1-\sum_{j=1}^{i-1}x_j \tag{3.20}$$

So using these quantities, we can rewrite our PDFs as:

$$f_i(x,Q^2)\ \longrightarrow\ \frac{1}{X}f_0\left(\frac{x}{X}\right) \tag{3.21}$$

where f_0 the original one-parton inclusive PDFs.

Now, requiring also the flavour conservation and taking into account the number of valence and/or sea quarks involved in the preceding MPI. We have now the full forms of the PDFs used for the $i-th$ MPI:

$$f_i(x,Q^2) = \frac{N_{fv}}{N_{fv0}}\frac{1}{X}f_{v0}\left(\frac{x}{X},Q^2\right) + \frac{a}{X}f_{s0}\left(\frac{x}{X},Q^2\right) + \sum_j \frac{1}{X}f_{cj0}\left(\frac{x}{X},Q^2\right) \tag{3.22}$$

$$g_i(x,Q^2) = \frac{a}{X}g_0\left(\frac{x}{X},Q^2\right) \tag{3.23}$$

where:

- $f_i(x,Q^2)$ ($g_i(x,Q^2)$) are the squeezed PDFs for quarks (gluons)
- N_{fv} the number of remaining valence quarks of the given flavour
- N_{fv0} the number of original valence quarks of the given flavour (for the proton we have $N_u = 2$, $N_d = 1$)
- f_{s0} the sea-quark PDF
- f_{cj} the companion PDF, this arise from the splitting $g \to q\overline{q}$ and a quark j is kicked out.

The factor a is defined to satisfy the total momentum sum rule.

3.2.4 Impact Parameter Dependence

The simplest hypothesis for the multiple interaction simulation, it is to assume the same initial state for all hadron collisions without dependencies on the impact parameter.

The more realistic scenario it is to include the possibility that each collision could be characterized by a different impact parameter b, where a small b value correspond to a large overlap between the two hadrons this is related to the probability of parton-parton interaction to take place.

It is neccesary to make some assumption on the matter distribution inside the proton. A possibility is to assume a spherically simmetric distribution inside a hadron at rest $\rho(\mathbf{x})\,d^3x = \rho(r)\,d^3x$. A Gaussian ansatz is the most simple choice but it appears to lead to a narrow multiplicity distribution and too little of a pedestal effect. So the coiche is a double Gaussian:

$$\rho(r) \propto \frac{1-\beta}{a_1^3}\exp\left\{-\frac{r^2}{a_1^2}\right\} + \frac{\beta}{a_2^3}\exp\left\{-\frac{r^2}{a_2^2}\right\} \tag{3.24}$$

where a fraction β of matter is contained in a radius a_2, and the rest in a larger radius a_1.

Now for a given matter distribution $\rho(r)$, the time-integrated overlap function of the incoming hadrons during the collision is given by:

$$\mathcal{O}(b) = \int dt \int d^3x\,\rho(x,y,z)\,\rho(x+b,y,z+t) \tag{3.25}$$

this is useful to quantify the effect of overlapping protons. The larger is $\mathcal{O}(b)$ the more probable are parton-parton scatters between the incoming protons.

So, these assumption change the so-far Poissonian nature of the framework

$$\mathcal{P}(\widetilde{n}) = \langle\widetilde{n}\rangle^{\widetilde{n}}\ \frac{e^{-\langle\widetilde{n}\rangle}}{\widetilde{n}!} \tag{3.26}$$

Now the request of at least one interactions and the introduction of an impact parameter b modify the probability distribution of interactions number from a Poissonian to a narrower one.

3.2.5 Parton rescattering

It is not necessary that the partons undergoing to a MPI are a different partons couple from the one scattered before. As shown in Fig. 3.2 MPI can also arise when a parton scatters more than once against partons from the other beam, this is call *parton rescattering*.

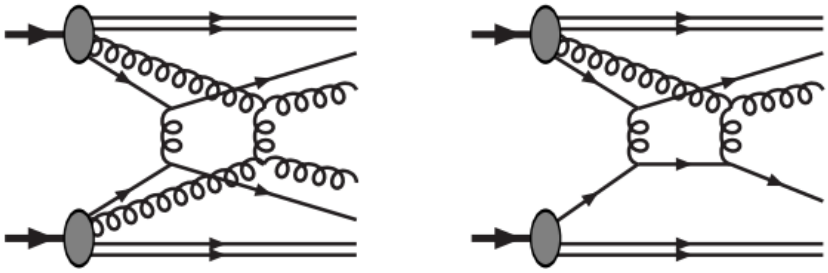

Figure 3.2: Add caption

We can have 3 type of MPI:

1. No ones of the partons that enter in the second scattering undergoes to another scatter before
2. Only one of the two partons have alredy been scattered
3. Both the partons have alredy been scattered before.

The second and the third are the rescatters the overall influence of rescatters in proton-proton interactions was estimated to be small respect to the first case with distinct $2 \to 2$ scatters.

The simulation of parton rescatters start from the evaluation of the parton density as:

$$f(x, Q^2) \quad \longrightarrow \quad \underbrace{f_{\text{rescaled}}(x, Q^2)}_{\text{hadron remnant}} + \underbrace{\sum_n \delta(x - x_n)}_{\text{scattered parton(s)}} \tag{3.27}$$

The δ take into account the scattered partons that have a fixed momentum fraction x_n. While the hadron remnant is still described by a continuous momentum density, rescaled to achieve momentum conservation:

$$\int_0^1 \left(f_{\text{rescaled}}(x, Q^2) + \sum_n \delta(x - x_n) \right) dx = 1 \tag{3.28}$$

3.2.6 Interleaving of Multiple Interaction and Parton Shower

As discussed above the MPI are simulated in `Pythia` following a decreasing p_T evolution. So we have that the total probability is given from the composition of the various contributions:

$$\begin{aligned} \frac{d\mathcal{P}}{dp_T} = &\left(\frac{d\mathcal{P}_{MPI}}{dp_T} + \sum \frac{d\mathcal{P}_{ISR}}{dp_T} + \sum \frac{d\mathcal{P}_{FSR}}{dp_T} \right) \\ &\times \exp\left\{ - \int_{p_T}^{p_T\, i-1} \left(\frac{d\mathcal{P}_{MPI}}{dp'_T} + \sum \frac{d\mathcal{P}_{ISR}}{dp'_T} + \sum \frac{d\mathcal{P}_{FSR}}{dp'_T} \right) dp'_T \right\} \end{aligned} \tag{3.29}$$

In Fig. 3.3 are shown 4 parton-parton interactions with their associated showers (ISR and FSR). The downward evolution correspond to read the graph from top to bottom. The first

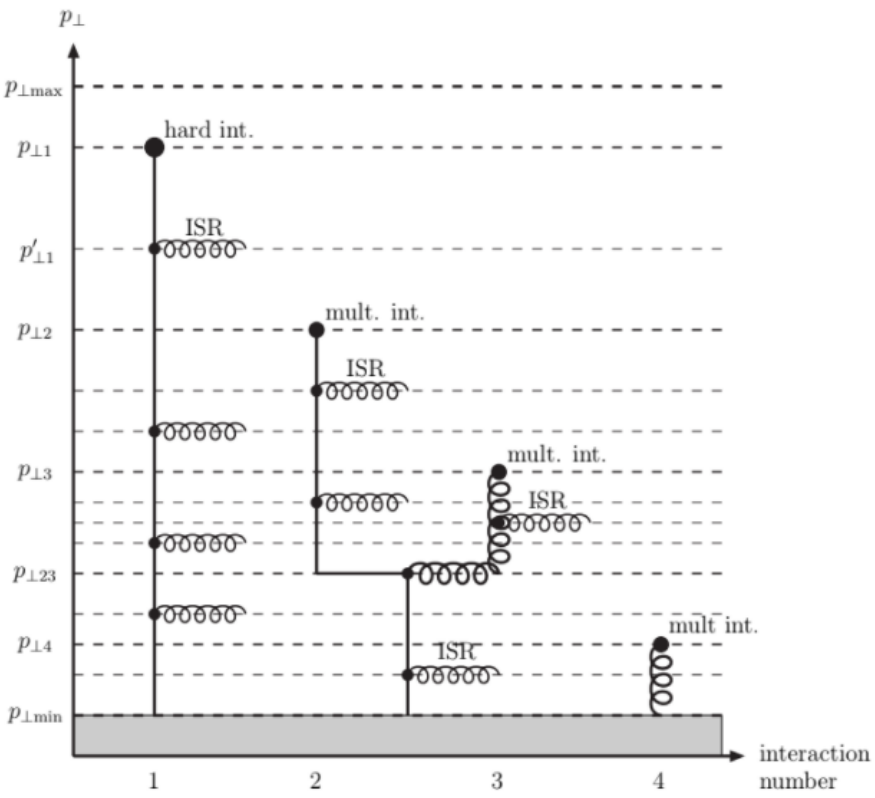

Figure 3.3: add caption

hard interaction occur at a scale $p_T = p_{T1}$ while the following ones at lower scales p_{T2}, p_{T3}, p_{T4}. Each interaction is associated with is radiation the first one occurs at $p_T = p'_{T1}$. The scatterings that occur at p_{T2} and p_{T3} are originating from the same mother parton.

This diagram is related to one of the two hadrons. The full event can be illustrated if a similar diagram is drawn for the other hadron and connected to the full black circles.

3.2.7 Beam Beam Remnants and primordial k_T

What is left after that the evolution is end? the evolution in p_T can create an arbitrary complicate final state.

This final state contains contributions from the scattered and unscattered partons that don't enter the p_T evolution. The last are the so called Beam Beam Remnants (BBR). BBR take into account the number of valence quark remaining and the number of sea quark required for the overall flavour conservation.

To ensure momentum conservation the BBR have to take all the remaining longitudinal momentum that is not extracted by the MPI initiators.

Primordial k_T

We have considered only the longitudinal momentum. in a real scenario partons inside the hadrons are fermions so are expected to have a non zero initial transverse momentum arising from the Fermi motion inside the incoming hadrons. This is denoted as "Primordial k_T" this is different from the transverse momentum derived from DGLAP shower evolution or from the hard interaction.

Based on Fermi motion alone, one would expect a value of the primordial k_T is estimate as:

$$k_T \simeq \frac{\hbar}{r_p} \approx \frac{0.2 \text{ GeV} \cdot \text{fm}}{0.7 \text{ fm}} \approx 0.3 \text{ GeV} \tag{3.30}$$

but for example to reproduce the data for the the p_T distributions of Z bosons produced in hadron–hadron collisions, one need a larger contribution. This phenomenon has not a satisfactory explanation. Until an explanation is found the idea is to consider a effective primordial k_T for the initiators larger than the one in Eq. 3.30.

In `Pythia` the primordial kT is assigned to initiators sampling a Gaussian distributions for p_x and p_y independently with variable width σ

$$\sigma(Q, \widehat{m}) = \frac{Q_{1/2}\,\sigma_{\text{soft}} + Q\,\sigma_{\text{soft}}}{Q_{1/2} + Q} \frac{\widehat{m}}{\widehat{m}_{1/2} + \widehat{m}} \tag{3.31}$$

Where Q is the hard-process renormalization scale for the main hard process and the p_T scale for subsequent MPI. σ_{soft}, σ_{hard} are the minimum and maximum width, $\widehat{m}$ is the invariant mass, while $Q_{1/2}$ and $\widehat{m}_{1/2}$ the halfway values between the two extremes.

3.2.8 Color Reconnection and Hadronization

The last important step at parton level is the color reconnection.

4. Observable to Study the Underlying Event

The UE are all the processes not associated with the primary hard scatter in an hadron-hadron collision.

All the process described in the previous section: initial- and final-state radiation, multiple interactions, and beam remnants and their interactions. These contribute to the Underlying Event (UE) in the proton-proton collision.

The most of the observable to study the UE are sensible only to the sum of these contributions and not to the single ones.

4.1 Minimum Bias Measurements and Underlying Event topology

A Minimum Bias (MB) measurement is a collection of inelastic events with a loose event selection. The event are collected requiring the minimal interaction with the detector (the smallest possible bias). The most of the interaction in MB observation are soft, $p_T \lesssim 2$ GeV. The study of the UE require at least one hard scattering presence.

To study the UE the topological structure of an hadron hadron collision is used. On an event-by-event analysis the direction of the leading object is used to define regions in the $\eta - \phi$ space. Where η is the pseudorapidity defined as $\eta = -\log\tan\left(\frac{\theta}{2}\right)$, while ϕ is the azimuthal angle in the $x - y$ plane. The last one is defined from the direction of the leading object as $\Delta\phi = \phi - \phi_{\text{leading}}$

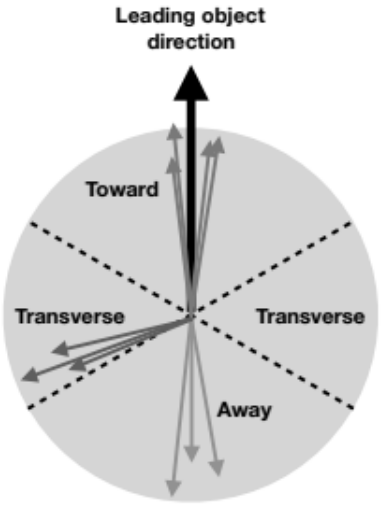

Region	
Toward	$\lvert\Delta\phi\rvert < 60°$
Away	$60° < \Delta\phi < 120°$
Transverse	$\lvert\Delta\phi\rvert > 120°$

Figure 4.1: ADD Caption

The regions classification is shown in Fig. 4.1, we have:

- **Toward region**: the region that contains the leading object, this region contains the most of the particle produced by the hard interaction.
- **Away region**: this region contains the objects that recoil against the leading object, also this region contains mostly the particles produced by the hard interaction.
- **Transverse regions**: the two transverse regions are the most sensitive to UE.

The transverse regions are also separated in:

– **TransMAX**: This is the transverse region that contains the *maximum* number of charged particles, or scalar p_T sum of charged particles. This regions includes both MPI and hard-process contamination.

– **TransMIN**: is the transverse region that contains the *minimum* number of charged particles, or scalar p_T sum of charged particles. This region is the most sensitive to MPI effects.